Single-nanoparticle electrophoretic mobility determination and trapping using active-feedback 3D tracking

Alexis Johnson and Kevin D. Welsher

Department of Chemistry, Duke University, Durham, NC 27708, USA

Abstract

Nanoparticles (NP) are versatile materials with widespread applications across medicine and engineering. Despite rapid incorporation into drug delivery, therapeutics, and many more areas of research and development, there is a lack of robust characterization methods. Light scattering techniques such as dynamic light scattering (DLS) and electrophoretic light scattering (ELS) use an ensemble-averaged approach to the characterization of nanoparticle size and electrophoretic mobility (EM), leading to inaccuracies when applied to polydisperse or heterogeneous populations. To address this lack of single-nanoparticle characterization, this work applies 3D Single-Molecule Active Real-time Tracking (3D-SMART) to simultaneously determine NP size and EM on a per-particle basis. Single-nanoparticle EM is determined by using active feedback to "lock on" to a single particle and apply an oscillating electric field along one axis. A maximum likelihood approach is applied to extract the single-particle EM from the oscillating nanoparticle position along the field-actuated axis, while mean squared displacement is used along the non-actuated axes to determine size. Unfunctionalized and carboxyl-functionalized polystyrene NPs are found to have unique EM based on their individual size and surface characteristics, and it is demonstrated that single-nanoparticle EM is a more precise tool for distinguishing unique NP preparations than diffusion alone, able to determine the charge number of individual NPs to an uncertainty of less than 30. This method also explored individual nanoparticle EM in various ionic strengths (0.25-5 mM) and found decreased EM as a function of increasing ionic strength, in agreement with results determined via bulk characterization methods. Finally, it is demonstrated that the electric field can be manipulated in real time in response to particle position, resulting in one-dimensional electrokinetic trapping. Critically, this new single-nanoparticle EM determination and trapping method does not require microfluidics, opening the possibility for the exploration of single-nanoparticle EM in live tissue and more comprehensive characterization of nanoparticles in biologically relevant environments.

Introduction

Nanoparticles (NPs) are important materials rapidly being incorporated into a wide range of scientific and engineering applications, such as diagnostics, imaging, and drug delivery.[1-2] Due to their widespread application, detailed characterization of NPs in various contexts is critical. Despite extensive research on nanomaterials, few nanotechnologies reach clinical trials and rarely achieve commercial success in contributing to human health, with the notable exception of lipid nanoparticle-based vaccines developed in response to the SARS-Cov-2 pandemic.[3-4] Challenges faced by nanomedicine are often rooted in the lack of robust characterization in complex biological environments. The abundance of various proteins and salts in biological sera leads to changes in the surface properties that may impact the transport of NPs to target sites, decrease cellular uptake of NPs, and even increase cytotoxicity and autophagic response.[4] NP characterization methods that faithfully report changes to surface properties are critical for developing and understanding successful nanomedicines, particularly *in vivo*.

Light-scattering-based techniques have become the workhorses of nanomedicine development. Dynamic light scattering (DLS) is a bulk technique, using scattered light from diffusing objects in dilute solutions, aided by an autocorrelation function, to measure the hydrodynamic radius of nanoscale particles. This technique is robust for reporting the ensemble-averaged radius of

particles in monodisperse solutions but faces many challenges with polydispersity.[5] The scattering signal from large particles or small aggregates can easily eclipse that from single molecules.[6] Biological solutions contain various proteins and other macromolecules that may induce NP aggregation, leading to a high degree of polydispersity and difficulties in assessing appropriate dosage, toxicological findings, and identifying therapeutic mechanisms of action.[7]

Measurement of size and aggregation state via DLS is only an indirect readout of the NP surface properties. Measurement of the electrophoretic mobility can reveal more detailed information about surface chemistry. Electrophoretic mobility (EM) is the behavior of colloidal particles in an external electric field and is highly sensitive to NP size, surface characteristics, and solubility. EM is often reported via the electrostatic surface potential or zeta potential (ZP) using Smoluchowshi's formula for rigid, spherical colloids.[8] EM is measured using electrophoretic light scattering (ELS), operating in the same fashion as DLS, but with the addition of an externally applied electric field. Brownian motion, or the "random walk" of particles in solution, is altered by the electric field to probe the surface properties of NPs. Both EM and ZP are used to assess colloidal stability, protein corona formation, and protein-nanoparticle interactions. For example, Santander-Ortega and coworkers used EM to assess the colloidal stability and adsorption of IgG antibodies on polymeric NPs at physiological pH to simulate a drug delivery system with targeting abilities.[9] Malburet *et al.* elucidated the physiochemical parameters of polydisperse lipid nanoparticles (LNP) used as a delivery system for mRNA vaccines by measuring EM and using it to calculate ZP and surface charge density.[10] Unfortunately, methods used to characterize EM in a biological context suffer from the same pitfalls as DLS. The EM reported is a product of an ensemble average that is likely to be biased towards large particles in solution, similar to DLS. The advancement of nanomedicines requires new, robust, and unbiased methodology.

There are critical shortcomings of ELS as an evaluation of NP surface properties. As an ensemble measurement, ELS struggles with accurately characterizing heterogeneous solutions, where critical sub-populations can be obscured. Single-particle approaches are key to capturing these potentially critical sub-populations and dynamics. To address this shortcoming, single-particle methods with the capability to measure EM and ZP have emerged in recent years. Both Choi *et al.*[11] and Oorlynck *et al.*[12] have introduced single-particle methods for nanoparticle characterization that specifically focused on measuring EM. They both use image-based particle tracking methods to monitor particle behavior along one axis in response to an electric field to measure EM in home-built microfluidics chambers. Image-based tracking often has a limited, predetermined observation volume, which is often a result of a limited axial range.[13] Even in shallow microfluidics chambers, this can lead to variation in EM measurement due to the axial position of a particle. Most importantly, the reliance on microfluidics means these methods often cannot be translated to *in situ* measurements of single-particle EM in the presence of live tissue.

While existing methods rely on microfluidics to confine particles to an observable volume, real-time 3D single-particle tracking (RT-3D-SPT) can lock onto individual particles as they diffuse over long 3D distances, collecting long trajectories of single NPs with millisecond or better temporal resolution. Importantly, this technique is easily translatable to complex biological settings. Here, we demonstrate that 3D Single-Molecule Active Real-Time Tracking (3D-SMART) is an ideal method for single NP EM determination.[14] 3D-SMART locks onto fluorescent polystyrene nanoparticles (PS NPs) in solution as they diffuse using active-feedback tracking (Fig. 1). A dynamic observation volume follows the particle of interest as it diffuses and uses the signal from a single-photon counting detector, removing the temporal limitations imposed by camera exposure and readout times in image-based tracking methods. Previously, 3D-SMART has been able to track viral contacts with the cell surface,[15] characterize *in situ* protein corona formation,[16] determine growth kinetics of single polymer particles in solution,[17] and characterize LNP diffusion

through mucus suspensions.[18] This technique has proven capable of extracting precise nanoparticle characteristics in complex environments. With the addition of an applied electric field, 3D-SMART provides a 3D trajectory at a kHz sampling rate, simultaneously revealing single particle parameters such as diffusion coefficient, hydrodynamic radius, and EM, which is new to this work.

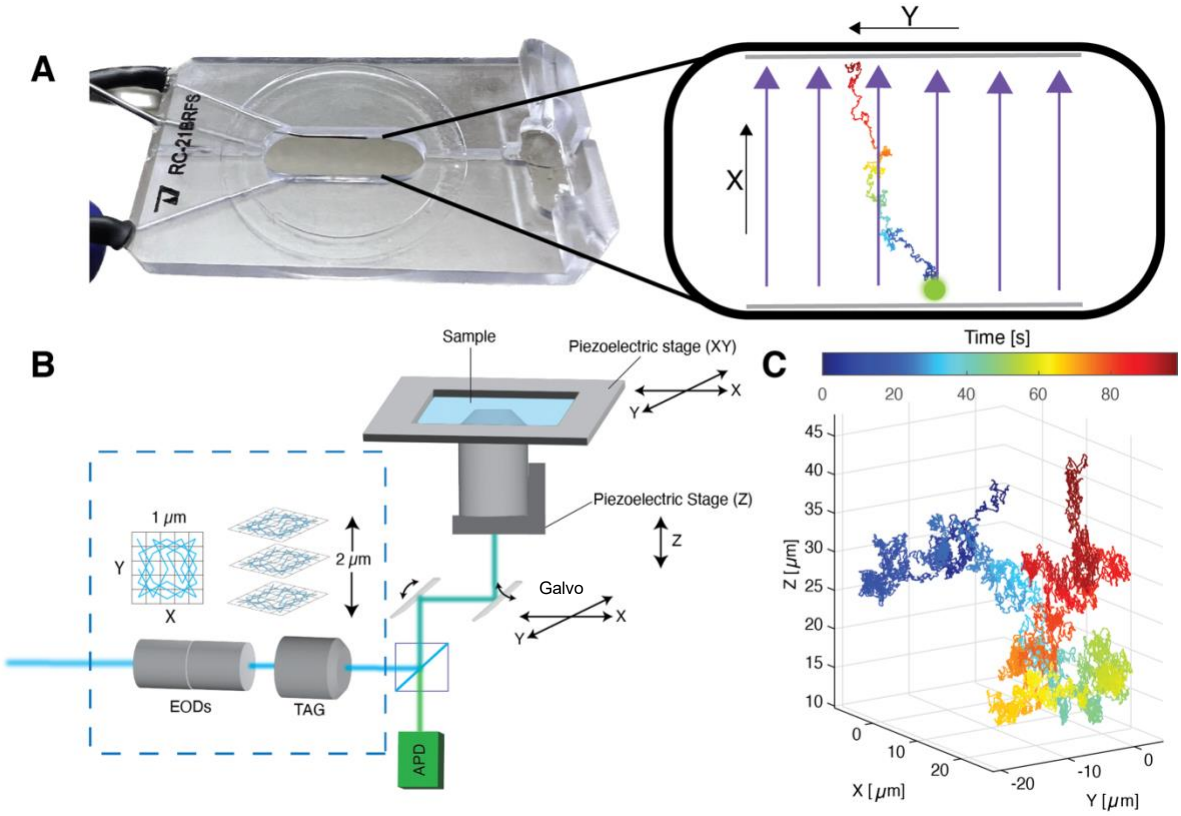

Figure 1: Experimental scheme for single-particle EM measurements. (A) Field-stimulation open-bath chamber. Inset: diffusing nanoparticle under applied electric field. (B) 3D-SMART microscope illustration. (C) Example 3D trajectory of a freely diffusing nanoparticle in water, captured by 3D-SMART.

Results and Discussion

Active-Feedback 3D Single-Particle Tracking with Electric Field Manipulation

3D-SMART achieves real-time tracking of single fluorescent nanoparticles through rapid position estimation within a 3D observation volume, which is then used as the input to a feedback loop that recenters the particle in the observation volume. The 3D volume is created by electro-optical deflectors (EODs) to deflect a 488 nm laser in X and Y in a knight's tour pattern[19] at 20 μsec per spot and 500 μsec for the entire 5 × 5 grid. Along the Z axis, the focus is deflected in a sine wave at ~70 kHz by a tunable acoustic gradient (TAG) lens. Together, the EODs and TAG lens create a rapid scan over a 1 × 1 × 2 μm scanning volume. Position estimates are made using photon arrival times recorded by the avalanche photodiode (APD) and a Kalman filter implemented on a field programmable gate array (FPGA, NI PCIe-7852R). The position estimate is fed into an

integral feedback controller to center the observation volume on the diffusing nanoparticle via piezoelectric nanopositioners or galvo scanning mirrors. In addition to the standard configuration of 3D-SMART, measurements of electrophoretic mobility require an applied electric field. Here, an electric field is applied using the analog output of the FPGA and is controlled via National Instruments LabVIEW software. For 3D-SMART, experimental conditions include a small sample volume (~300 µL) in an open bath chamber with parallel platinum electrodes capable of field stimulation (Warner Instruments RC-21BRFS, Fig. 1A). This chamber houses freely diffusing NPs in solution for the duration of the experiment under various field stimulation modes, allowing Brownian motion of PS NPs in water to be recorded in real-time by 3D-SMART (Fig. S1). The 18 × 6.3 mm chamber makes it very unlikely for NPs in the dilute solution to encounter the chamber walls. Any alterations in diffusive motion or electrophoretic mobility due to contact with sidewalls are assumed to be negligible.

The maximum applied voltage across the sample for the experiments below is 2 V, corresponding to a field strength of 3.2 V/cm. The voltage was set at a maximum after testing the response of the 3D-SMART system to different voltages ranging from 1 to 10 V, measuring the resulting drift velocity, and comparing it to the expected outcome (Fig. S2). At voltages greater than 4 V (6.4 V/cm), the measured drift velocity greatly deviated from the expected value. This is likely due to position estimation inaccuracies at high velocities.

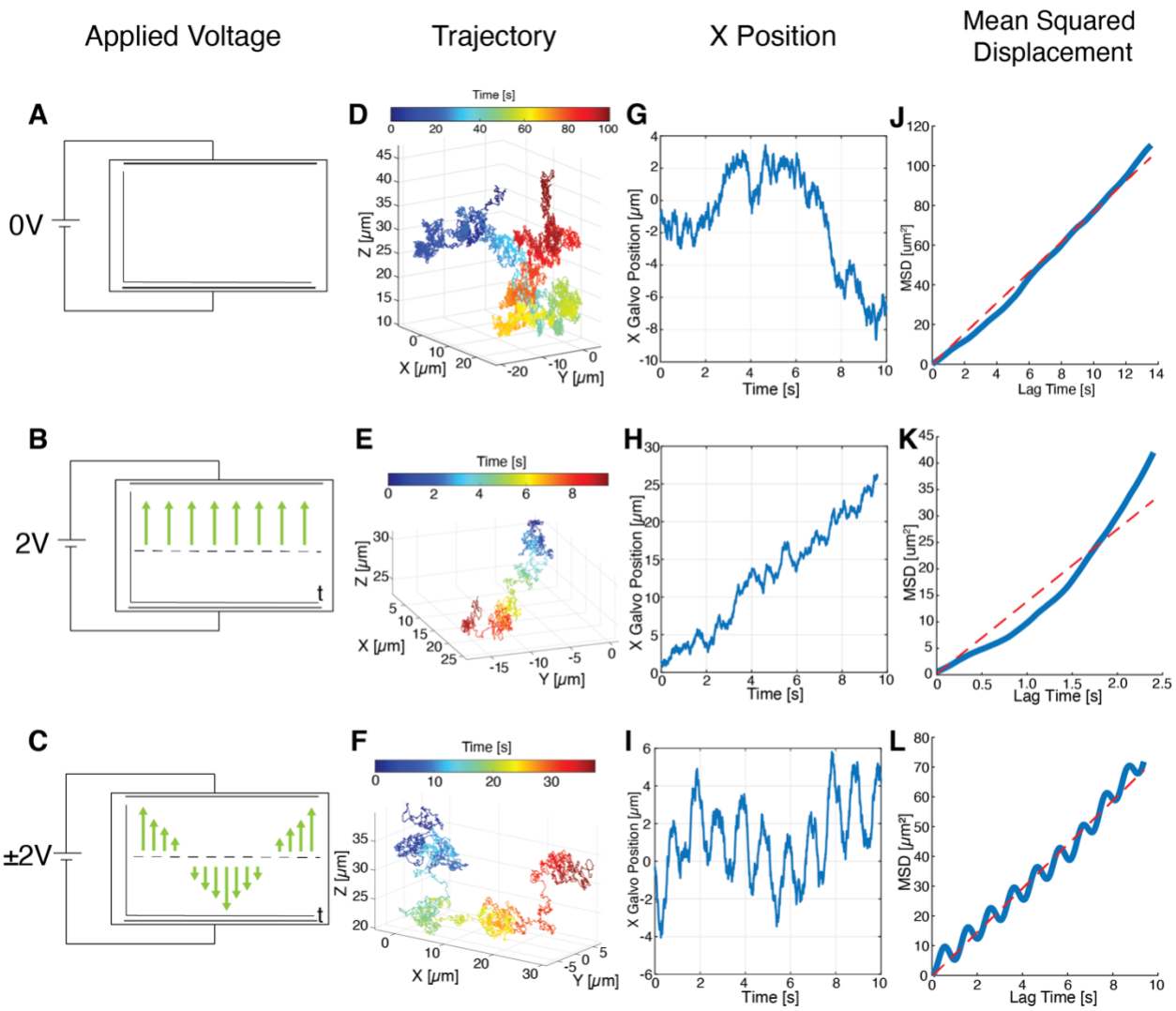

Figure 2: Three-dimensional motion of nanoparticles in solution under various applied voltage conditions. (A-C) Illustration depicting the voltage conditions applied along the X direction: 0V, constant application of +2 V, and sinusoidal oscillation between +2 V and -2 V at a frequency of 1 Hz. (D-F) Representative 3D trajectories of 196 nm carboxyl-functionalized PS NPs diffusing under the field conditions specified in (A-C). (G-I) X position of nanoparticles versus time under the field conditions specified in (A-C). (J-L) Mean squared displacement versus lag time of particles under the field conditions specified in (A-C).

Figure 2A-C demonstrates the modes of voltage application utilized in the current study: zero applied voltage corresponding to Brownian motion (0 V, Fig 2A), constant voltage (+2 V, Fig 2B), and oscillating voltage between -2 V and +2 V at a frequency of 1 Hz (± 2 V, Fig. 2C). In the zero-field condition, Brownian motion is observed, as shown for a 196 nm carboxyl-modified PS NP diffusing for approximately 90 seconds in Figure 2D. The 3D trajectories (Fig. 2D-F), which are extracted from the readout of the piezoelectric nanopositioners and galvo mirrors, show the movement of the particle overall. The X-position, which corresponds to the axis of field stimulation, is isolated from the trajectory (Fig. 2G-I) for mean squared displacement (MSD) analysis (Fig. 2J-L) to illustrate the effect of field actuation on particle motion. For simple Brownian motion, the slope of the MSD plot versus lag time provides the diffusion coefficient, which in turn can be used to determine the hydrodynamic radius via the Stokes-Einstein relation (Equations S2 and S3).

MSD plots for the non-actuated axes (Y and Z) are used to accurately determine the hydrodynamic radius of the particle and aggregation state in the presence or absence of the applied field (Fig. S3-7).

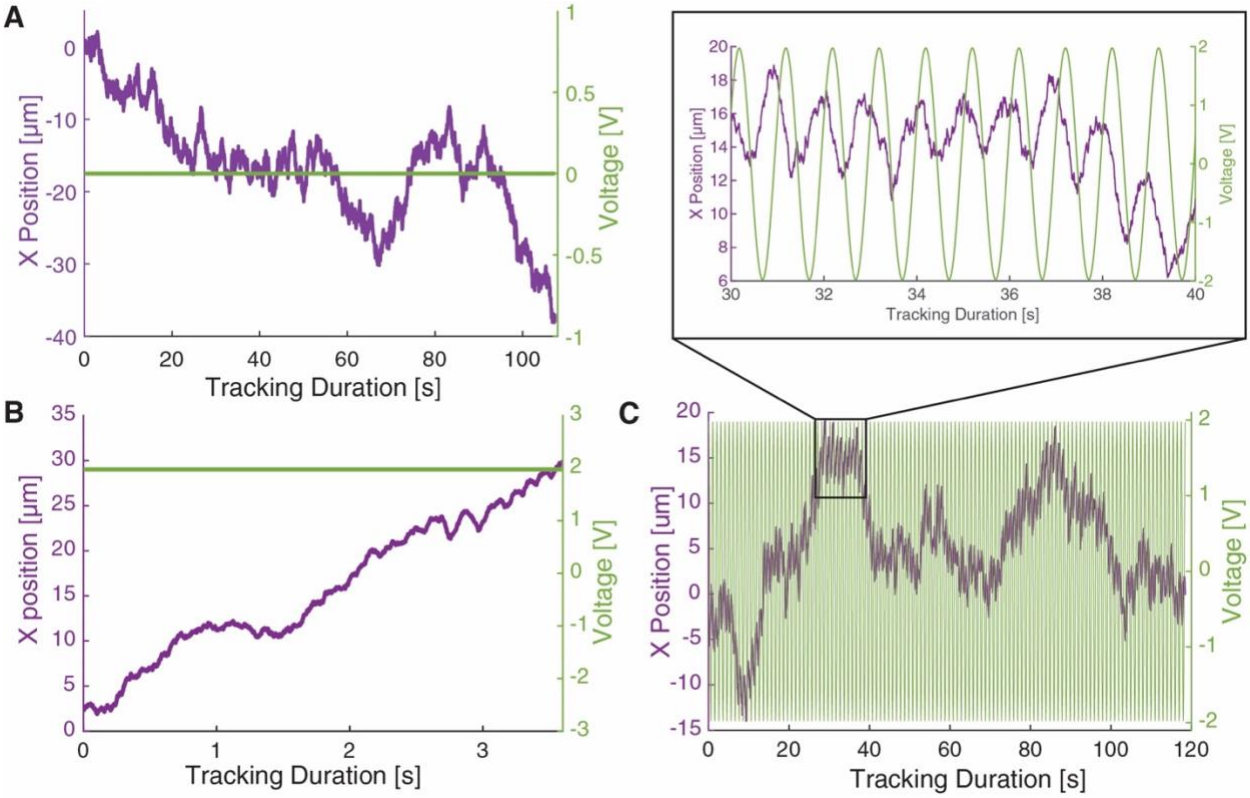

Figure 3: Directed particle motion in the X direction due to electric field stimulation. Nanoparticle X position with (A) zero applied voltage, (B) constant applied voltage, and (C) oscillating applied voltage.

When applying an electric field along the X-axis, the behavior of a 196 nm PS NP undergoes noticeable changes along the manipulated axis. The data above clearly establishes that the expected Brownian motion is perturbed in response to the applied electric field. Upon examining the overlay of the applied voltage and the position of the particle along the field axis, it can be observed that the particle moves in direct response to the field (Fig. 3). In contrast to the zero-field condition which shows Brownian motion (Fig. 3A), a constant voltage of +2 V along the X direction of the sample chamber “pushes” the particle in one direction correlating with the applied electric field (Fig. 3B). The applied field results in a deviation from Brownian motion, which is clearly observed in the non-linear slope of the MSD plot (Fig. 2K). The MSD curve slopes upwards with increased lag time, taking on a convex shape. This shape is characteristic of particle drift or directed motion, which strongly suggests that the particle is drifting due to the constant applied voltage. The relationship between the applied field and particle motion can be seen most clearly in the oscillating field case (Fig. 3C). A tight correlation is seen between the 1 Hz applied field and the particle position. This is further confirmed using a Welch’s power spectral density estimate performed on the X position data (Fig. S8) as compared to the non-actuated Y axis. The MSD takes on an unusual shape that is not one of the typical behaviors used to classify the motion of molecules in solution (Brownian, directed, or confined motion). The MSD versus lag time takes on the same oscillating behavior as the applied field. The presented data makes it apparent that

3D-SMART can track the manipulated position of NPs in solution in response to an electric field. The response of the particle position due to the change in voltage is the basis for measuring the electrophoretic mobility. ee**Calculating electrophoretic mobility** eThe electrophoretic mobility can be related to the experimentally measured drift velocity (u) and the applied electric field (E) via Equation 1. Electrophoretic mobility can also be expressed in terms of voltage (V) and chamber length (d) via Equation 2.

$$\mu = \frac{u}{E} \quad (1)$$

$$V = \frac{d \times u}{\mu} \quad (2)$$

The displacement of the particle along the X-axis of the tracking volume is calculated based on the coordinate data recorded via 3D-SMART to calculate the electrophoretic mobility of the particle. The voltage applied by the FPGA and the distance between the platinum wires (d) were used to calculate E. The probability density of observing a particle displacement, Δx, after a time τ with diffusion coefficient D and drift velocity u, follows a Gaussian probability distribution.

$$P\ (\Delta x; u, D) = \frac{1}{\sqrt{4\pi D\tau}} \exp\left(-\frac{(\Delta x - u\tau)^2}{4D\tau}\right) \quad (3)$$

Under the conditions where a constant drift velocity is expected (under constant voltage), the mean displacement for a given τ is sufficient to extract the EM. However, this will yield an EM of zero for an oscillating potential. To account for this, we apply a maximum likelihood approach to extract the EM given a time-varying potential. The log-likelihood, L, of a particular u_i and D given a set of observed displacements Δx_i is

$$L(\mu, D; \Delta x_i) = \sum \ln\left(\frac{1}{\sqrt{4\pi D\tau}}\right) - \left(\frac{(\Delta x_i - u\tau)^2}{4D\tau}\right) \quad (4)$$

$$L(\mu, D; \Delta x_i, d, V_i) = \sum \ln\left(\frac{1}{\sqrt{4\pi D\tau}}\right) - \left(\frac{\left(\Delta x_i - \frac{\mu V_i}{d}\tau\right)^2}{4D\tau}\right) \quad (5)$$

Finding the maximum of Equation 5 can yield the maximum likelihood estimate (MLE) of both μ and D. In the work described below, the value of D is calculated from the mean-squared displacement along the non-actuated axis (Y), and a one-dimensional log-likelihood is used to find the value of the drift velocity. The MLE and 95% confidence intervals are reported for all data reported below.

Precision of electrophoretic mobility measurement scales with trajectory duration

After collecting trajectories under the influence of an applied field and calculating the underlying EM, the data were next evaluated to determine the factors that relate to the precision of the extracted parameters. It was observed that the trajectory duration is the critical factor in EM precision. To reach a relative uncertainty of 10%, single-particle trajectories must exceed 20 seconds in tracking duration. Trajectories collected by 3D-SMART are occasionally short (<20 seconds) because of particle dimness, diffusion speeds beyond microscope tracking capabilities, or reaching a physical limit (encountering the edge of the stage or galvo range). As the cumulative tracking duration increases, the relative uncertainty of the calculated EM decreases, hitting ~10%

at 20 seconds and ultimately reaching 2.2% relative uncertainty at 180 seconds (Fig. 4A). Given this requirement for trajectory duration, the oscillating field approach is preferred over the constant field approach. Under constant field, particles will quickly drift across the active tracking range, reducing the observation time. The oscillating field gives no net bias on the particle's position, enabling longer observation. The majority of trajectories in an oscillating field (79 out of 102) meet this cut-off (Fig. 4B). Trajectories shorter than 20 seconds were excluded from further analysis, and the average relative uncertainty of retained oscillating field trajectories at 20 seconds is 11%.

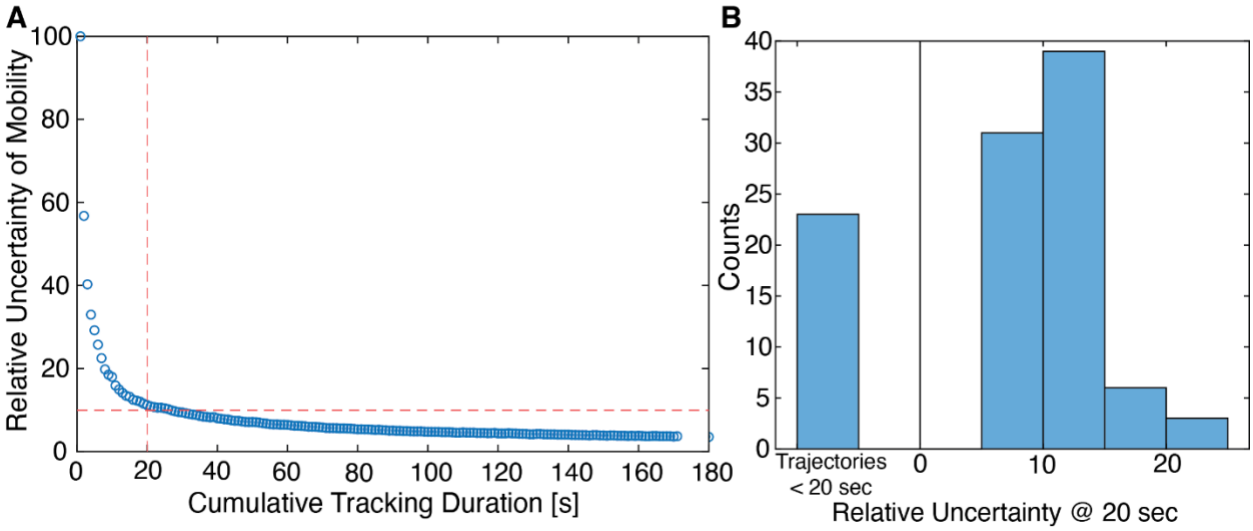

Figure 4: Relative EM uncertainty versus trajectory duration. (A) Relative uncertainty of electrophoretic mobility for 196 nm carboxyl-functionalized PS NPs calculated at each second of continuous tracking. The dotted red line denotes the desired cutoff criteria: 20 seconds of single particle tracking (vertical), and 10% relative uncertainty of measurement (horizontal). (B) Histogram of relative uncertainty values reached for individual trajectories at 20 seconds of tracking (N = 102).

Single-nanoparticle EM distinguishes particles by both size and surface charge

Aside from environmental factors, which are discussed below, the size and charge of the particle itself determine the magnitude and sign of the EM. Here, active-feedback single-nanoparticle EM was applied to two different types of NPs: unfunctionalized polystyrene (PS) and carboxyl-functionalized polystyrene (COOH-PS). Two sets of unfunctionalized PS NPs were measured with manufacturer-reported diameters of 190 nm and 194 nm. Under the oscillating electric field, each trajectory returns both the EM (from the field-actuated X-axis) and the diffusion coefficient (via MSD of the non-actuated Y-axis). The measured diffusion coefficients were $2.4 \pm 0.7 \times 10^{-12}$ m^2/s and $2.3 \pm 0.8 \times 10^{-12}$ m^2/s for 190 and 194 nm PS NPs, respectively. The distributions associated with these mean values are used to calculate the nanoparticle radius to monitor aggregation in solution. Although some NPs have a radius larger than what is expected, there is no increase in intensity for these larger particles. From this, we assume the population recorded only contained single nanoparticles. According to a t-test, there is no statistically significant difference between the measured diffusion coefficients of these two single-nanoparticle datasets, meaning it is not possible to differentiate these very similar populations of NPs via MSD analysis alone. In contrast, the measured values of EM were able to distinguish these two otherwise identical populations. The measured EM for these two types of PS NPs were $-3.11 \pm 0.6 \times 10^{-8}$ and $-3.31 \pm 0.3 \times 10^{-8}$ $m^2V^{-1}s^{-1}$, respectively. While there is a strong overlap of calculated mobilities within these two

populations (Fig. 5), the EM measurement is able to distinguish between these two types of NPs ($p < .005$). Although there is only a 4 nm difference in the diameter between the two types of PS NPs, their difference in reported EM is consistent with a fundamental picture of EM. Even when unfunctionalized, polystyrene carries a negative charge. The larger diameter leads to a larger surface area to interact with ions in solution. In the presence of an electric field, the species with the higher overall surface charge will react more strongly to the field, contrary to what is expected for free diffusion. COOH-PS NPs were used to test the effect of surface charge on the EM. The first COOH-PS NPs used haave a manufacturer-reported diameter of 196 nm. For these NPs, the measured EM is $-3.91 \pm 0.6 \times 10^{-8}$ $m^2V^{-1}s^{-1}$ (mean ± s. d.), an increase in magnitude of 0.6 to 0.8 $\times 10^{-8}$ $m^2V^{-1}s^{-1}$ compared to unfunctionalized PS NPs of similar size. The increase in negative charge on the surface due to the carboxyl groups is expected to increase the overall magnitude of EM due to the increase in surface potential. Surface charge contributes to the magnitude of EM, and this is reflected in the single-particle EM extracted by 3D-SMART. Replication of EM measurements for 196 nm COOH-PS NPs also provides insight into the precision of this method. The replicates of single-nanoparticle determination of EM for 196 nm COOH-PS NP yielded mean (± s. d.) EM values of $-3.1 \pm 0.5 \times 10^{-8}$ $m^2V^{-1}s^{-1}$ and $-3.7 \pm 0.5 \times 10^{-8}$ $m^2V^{-1}s^{-1}$ (Fig. S9). The effect of nanoparticle size on EM was investigated using 102 nm COOH-PS NPs. For the 102 nm COOH-PS NP, the measured EM is $-3.5 \pm 0.4 \times 10^{-8}$ $m^2V^{-1}s^{-1}$. The lower EM values, compared to the other carboxyl-functionalized PS NPs, are likely due to the difference in size. The smaller NP has a smaller surface area, decreasing the available surface area for functional groups on the surface. Less total surface charge would have a weaker reaction to the applied electric field. When measuring the EM of these smaller NPs, significant sample-to-sample variance was observed. Multiple datasets were collected for these NPs and yielded very distinct results. The mean EM (± s. d.) were $-2.92 \pm 0.5 \times 10^{-8}$, $-3.81 \pm 0.4 \times 10^{-8}$ and $-1.57 \pm 0.6 \times 10^{-8}$ $m^2V^{-1}s^{-1}$ (Fig. S10), dramatically increased sample-to-sample variance compared to the larger COOH-PS NPs. It was observed that the EM value could change as a function of time after dilution from the stock solution. Older dilutions showed EM values near -1.57×10^{-8} $m^2V^{-1}s^{-1}$, corresponding to a ZP of -22 mV, close to the cut-off for a stable colloidal suspension. This near instability was reflected in an increase in the number of aggregates detected in the solution, as determined via MSD. These data show the power of this single-nanoparticle EM method to extract subtle changes in surface chemistry.

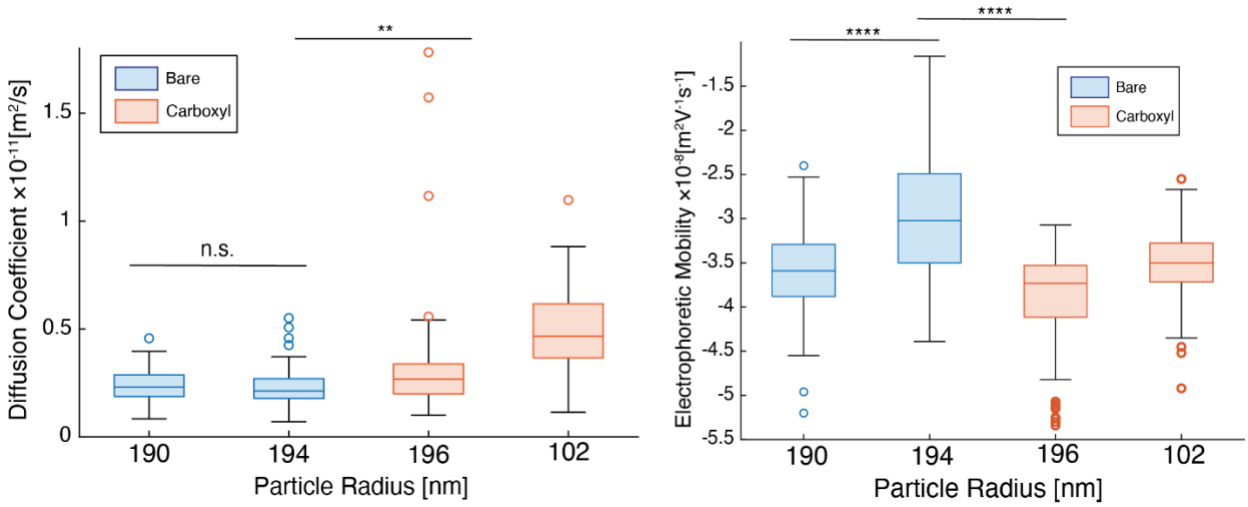

Figure 5: Electrophoretic Mobility and Diffusion Coefficients of various sizes and surface functionalities of PS NPs. (A) Real-time single-nanoparticle determined diffusion coefficient of

polystyrene nanoparticles. (B) Real-time single-nanoparticle determined EM of polystyrene nanoparticles. * = p<0.05, ** = p<0.01, ***=p<0.001, ****=p<0.0001

Ionic strength

There are many factors that affect the EM of NPs in solution. The EM of an individual NP reflects its environment, communicating the effective electric field in solution, availability of charge species in solution, and even solubility. One critical parameter that affects EM is ionic strength. Electrolytes affect the local electric field strength and alter NP mobilities. For example, the addition of electrolytes such as NaCl into solution changes the ionic strength as well as the Debye length of the particle (Table S1). Here, ionic strengths ranging from 0.25-5 mM were used to test the effect of electrolytes on single-particle EM. As shown in Figure 6A, an increase in ionic strength led to a consistent decrease in EM for 196 nm COOH-PS NPs. This agrees with previous studies that show a decrease in EM with increasing ionic strength.[20-21]

From the Debye-Hückel model, it is known that the Debye length of a particle is dependent on the ionic strength of the solution. Particles in solution are surrounded by an uneven distribution of ions and counterions in solution that constitute the Debye-Hückel ion cloud. The Debye length (κ^{-1}) is given by:

$$\kappa^{-1} = \left(\frac{\varepsilon_r \varepsilon_0 k_B T}{2 N_A e^2 I}\right)^{\frac{1}{2}} \quad (6)$$

Here N_A is Avogadro's number, e is the elementary charge, and I is the ionic strength. Higher ionic strength thins the electric double layer.[22] This is apparent from the effective charge of the double layer (Z_{eff}) as a function of EM at different solvent conditions (Fig. 6B).

$$Z_{eff} = \mu_E (6\pi\eta R_s) \quad (7)$$

The EM is dependent on the Z_{eff} of the particle because it is closely tied to the surface charge of the nanoparticle. As the electrolyte concentration in solution increases (higher ionic strength), the counterions in solution become more tightly associated with the particle's surface. The negative surface charge of the particle is increasingly screened by positive ions, causing the overall charge number to decrease as seen in Figure 6B. The valence charge number (Z) reflects this change and can be determined by dividing Z_{eff} by the elementary charge of an electron (e). The charge number is calculated for each individual NP based on the behavior seen in the trajectory as it is affected by the electric field.

$$z = \frac{Z_{eff}}{e} \quad (8)$$

The lowered surface charge leads to a weaker reaction to the electric field, resulting in a lower EM. We demonstrate here that in addition to EM, the charge number of individual NPs can be precisely measured by this new method (Table S2). For the included ionic strength range, the mean charge numbers (± s.d.) were -369±199, -227±77, -126±63, -74±29 and -39±24, respectively, as ionic strength increases. The mean uncertainty in charge number (± s. d.) for each population is 25±9, 22±6, 22±7, 23±10 and 24±8. Across all ionic strengths explored, the valence charge number of individual nanoparticles can be determined within less than 30 units, demonstrating the precision of this method to determine the charge of a single nanoparticle.

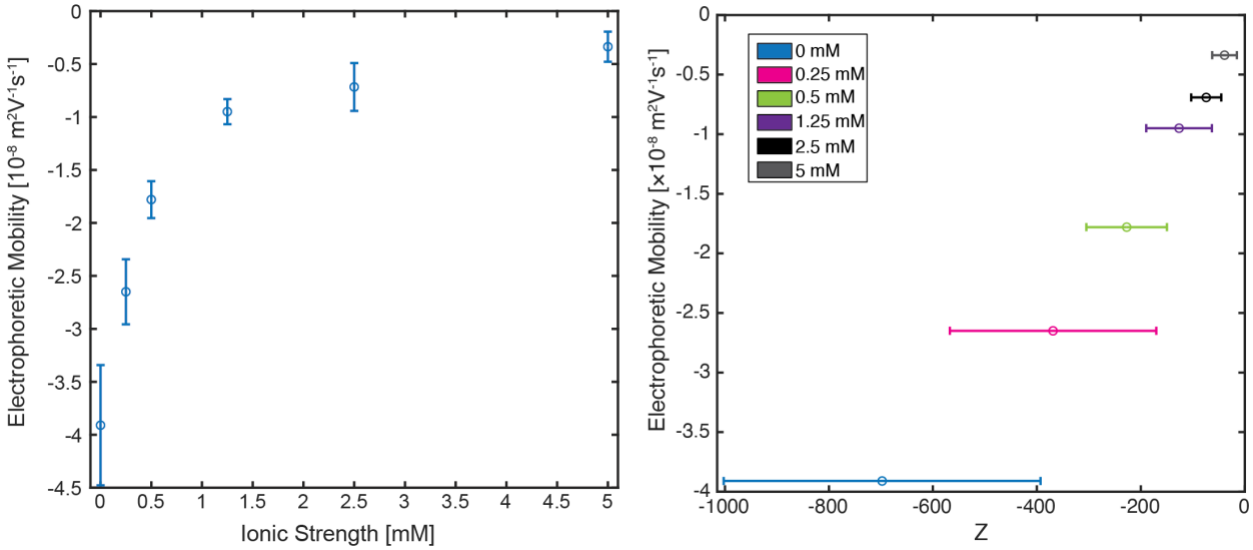

Figure 6: Ionic Strength dependence of single-particle EM. (A) EM of 196 nm carboxyl functionalized polystyrene nanoparticles vs ionic strength for 0-5 mM NaCl. (B) EM versus calculated charge number in NaCl solution. For both plots, error bars represent the standard deviation of the population.

Real-time particle manipulation with active-feedback field stimulation

A major difference between the active-feedback approach shown here and prior single-particle EM measurements is the real-time measurement of the particle position, which opens the possibility for real-time actuation of particles in solution. In previous work, the anti-Brownian electrokinetic (ABEL) trap has been able to trap single molecules in solution using electrokinetic feedback and microfluidics.[23-25] The work presented here provides a foundation for single-particle trapping without the use of microfluidics, more closely mimicking the native environment for single molecules. To demonstrate this, a simple feedback scheme was applied to maintain the position of a single particle in solution in one dimension. An arbitrary position within the sample was selected. When the particle was measured to be on one side of the boundary, +2 V was applied to push the particle back to the selected position. On the other side of the boundary, -2 V was applied. The results of this simple confinement scheme are shown in Figure 7. Despite the simplicity of the employed feedback scheme, the 110 nm COOH PS NP is able to be confined to within 1.38 μm (s.d., Fig. 7c), a dramatic confinement compared to the non-actuated Y-axis (Fig. 7d). The approach demonstrated here is a proof of principle that single nanoparticles can be manipulated in solution in real-time without the need for microfluidics. With an appropriately designed sample chamber with field stimulation along all three axes, arbitrary control should be possible for a wide range of nanoscale objects in complex biological systems.

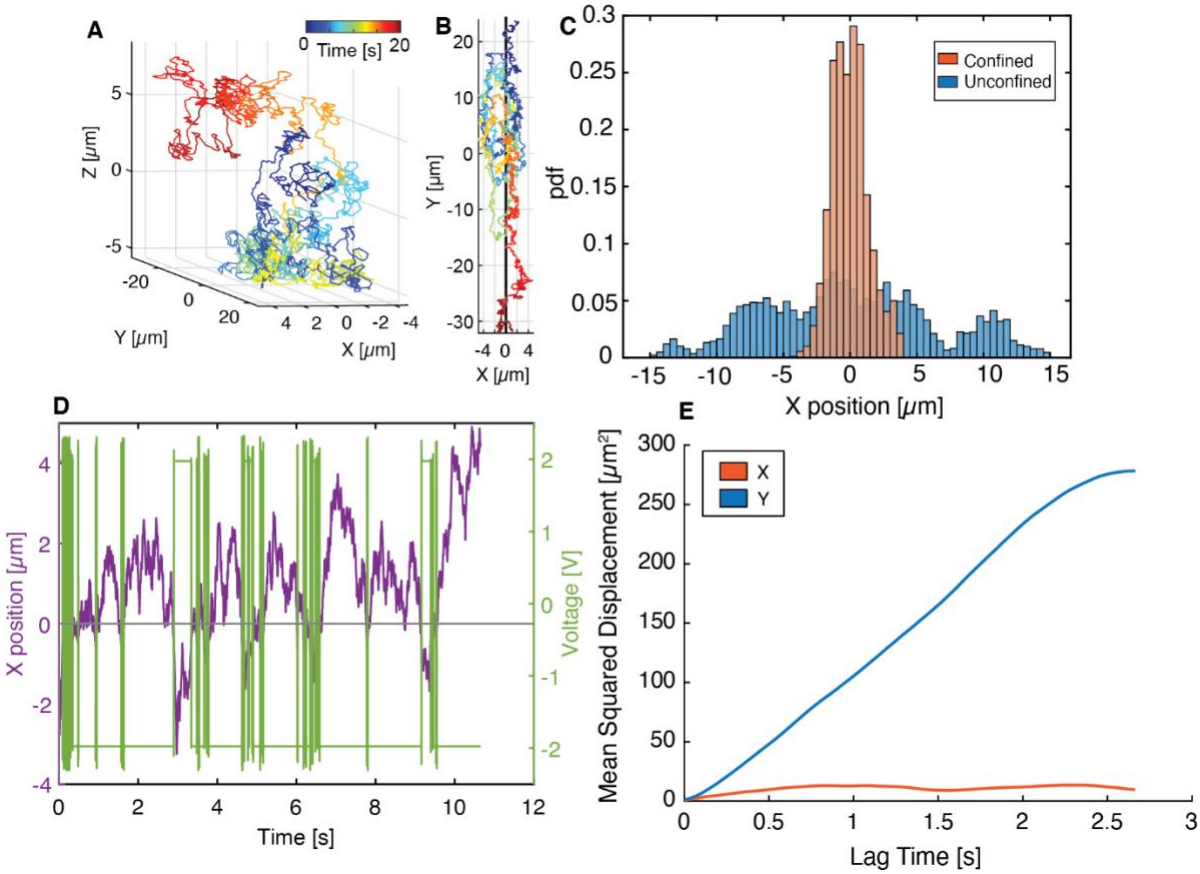

Figure 7: One-dimensional nanoparticle confinement via electrokinetic feedback. (A) 3D trajectory of 110 nm nanoparticle with electrokinetic feedback. (B) XY view of particle confinement trajectory using ±2 V feedback. (C) X position distribution of unconfined and confined particles. (D) Particle confinement of X position (blue) due to electrokinetic feedback (orange) with 40 μm boundary (black). (E) 1D MSD of directed motion along X-axis (blue) and free diffusion along the Y axis (blue).

Conclusion

The single-nanoparticle EM demonstrated here has a myriad of future potential applications, most of which involve measuring EM in complex environments. Future expansion of this new technique to biological environments will require overcoming several potential obstacles. The first is the conductivity of buffer solutions used or present in most biological systems (e.g. phosphate buffered saline). As the buffer conductivity increases, higher currents will be required to reach the same field strength. Careful consideration of how the present electrolytes contribute to redox reactions and heating of solution at increased ionic strengths will be critical. The second issue going forward is the decreased observation time of 3D-SMART as the diffusive speed of the probe increases. In its current state, 3D-SMART can track ~1 kB double-stranded DNA for several seconds.[26] This does not meet the 20-second tracking duration threshold demonstrated above. It is possible that the 20-second limit corresponds to a threshold number of oscillations needed to precisely measure the EM. Further exploration of the optimal frequency will be beneficial in the future as species of interest become smaller and diffuse more rapidly.

In the future, it should also be possible to take advantage of 3D-SMART's ability to be paired with concurrent imaging techniques (3D-TrIm)[15] and measure how the EM of nanoparticles, the protein corona, or even viruses change as they come in close proximity to cells. It should also be possible to measure the surface charge density of nanoparticles in these environments (Table S1). Surface charge density has been used in previous studies to assess nanoparticles as viable drug and gene carriers.[27-29] Real-time measurement of surface charge density and nanoparticle behavior in a cellular environment could give valuable insight into drug delivery and therapeutic design. Without reliance on microfluidics, translating this method to accommodate live tissue can be done with few adjustments to the experimental setup.

Here, we have demonstrated that 3D-SMART enables *in situ* electrophoretic mobility determination of single nanoparticles, with single nanoparticle charge calculated to within 30. Importantly, the size of the nanoparticle is simultaneously extracted. This means that any level of aggregation within solution, which in ensemble methods skews the reported values for particles in solution, is not a problem for this method as aggregates are easily discerned via MSD analysis. In contrast to prior works on single-nanoparticle EM extracting EM from single nanoparticles, the work described above does not require microfluidics, making expansion to complex biological samples possible. Furthermore, the real-time nature of 3D-SMART makes active electrophoretic confinement of a single nanoparticle possible, shown here for the first time without the use of microfluidics. This suggests that 3D confinement and manipulation will be possible in future work with an appropriately constructed sample chamber. Being able to precisely control and manipulate nanoscale objects will open new lines of investigation across the biological sciences.

Acknowledgments
We acknowledge financial support from the National Institute of General Medical Sciences of the National Institutes of Health under award number R35GM124868 (K.D.W.). This material is based upon work supported by the National Science Foundation Graduate Research Fellowship Program under Grant No. DGE 2139754 (A.J.).

References

(1) Allen, T. M.; Cullis, P. R. Drug Delivery Systems: Entering the Mainstream. *Science* **2004**, *303* (5665), 1818-1822. DOI: doi:10.1126/science.1095833.
(2) Lee, D.-E.; Koo, H.; Sun, I.-C.; Ryu, J. H.; Kim, K.; Kwon, I. C. Multifunctional nanoparticles for multimodal imaging and theragnosis. *Chemical Society Reviews* **2012**, *41* (7), 2656-2672, 10.1039/C2CS15261D. DOI: 10.1039/C2CS15261D.
(3) Attia, M. A.; Essa, E. A.; Elebyary, T. T.; Faheem, A. M.; Elkordy, A. A. Brief on recent application of liposomal vaccines for lower respiratory tract viral infections: From influenza to COVID-19 vaccines. *Pharmaceuticals* **2021**, *14* (11), 1173.
(4) Lim, S. H.; Wong, T. W.; Xian, T. W. Overcoming colloidal nanoparticle aggregation in biological milieu for cancer therapeutic delivery: Perspectives of materials and particle design. *Advances in Colloid and Interface Science* **2024**, 103094. DOI: https://doi.org/10.1016/j.cis.2024.103094.
(5) Bhattacharjee, S. DLS and zeta potential – What they are and what they are not? *Journal of Controlled Release* **2016**, *235*, 337-351. DOI: https://doi.org/10.1016/j.jconrel.2016.06.017.
(6) Eleamen Oliveira, E.; Barendji, M.; Vauthier, C. Understanding Nanomedicine Size and Biological Response Dependency: What Is the Relevance of Previous Relationships Established on Only Batch-Mode DLS-Measured Sizes? *Pharmaceutical Research* **2020**, *37* (8), 161. DOI: 10.1007/s11095-020-02869-x.
(7) Wills, J. W.; Summers, H. D.; Hondow, N.; Sooresh, A.; Meissner, K. E.; White, P. A.; Rees, P.; Brown, A.; Doak, S. H. Characterizing Nanoparticles in Biological Matrices: Tipping Points in

Agglomeration State and Cellular Delivery In Vitro. *ACS Nano* **2017**, *11* (12), 11986-12000. DOI: 10.1021/acsnano.7b03708.
(8) Kuo, Y.-C.; Lin, T.-W. Electrophoretic Mobility, Zeta Potential, and Fixed Charge Density of Bovine Knee Chondrocytes, Methyl Methacrylate− Sulfopropyl Methacrylate, Polybutylcyanoacrylate, and Solid Lipid Nanoparticles. *The Journal of Physical Chemistry B* **2006**, *110* (5), 2202-2208.
(9) Santander-Ortega, M.; Bastos-González, D.; Ortega-Vinuesa, J. Electrophoretic mobility and colloidal stability of PLGA particles coated with IgG. *Colloids and Surfaces B: Biointerfaces* **2007**, *60* (1), 80-88.
(10) Malburet, C.; Leclercq, L.; Cotte, J.-F.; Thiebaud, J.; Bazin, E.; Garinot, M.; Cottet, H. Size and Charge Characterization of Lipid Nanoparticles for mRNA Vaccines. *Analytical Chemistry* **2022**, *94* (11), 4677-4685. DOI: 10.1021/acs.analchem.1c04778.
(11) Choi, M. H.; Hong, L.; Chamorro, L. P.; Edwards, B.; Timperman, A. T. Correction: Measuring the electrophoretic mobility and size of single particles using microfluidic transverse AC electrophoresis (TrACE). *Lab on a Chip* **2024**, *24* (1), 148-148.
(12) Oorlynck, L.; Ussembayev, Y. Y.; Cid, I. A.; Fraire, J.; Hinnekens, C.; Braeckmans, K.; Strubbe, F. Laser-Scanning Microscopy for Electrophoretic Mobility Characterization of Single Nanoparticles. *Particle & Particle Systems Characterization* **2023**, *40* (1), 2200152. DOI: https://doi.org/10.1002/ppsc.202200152.
(13) Hou, S.; Johnson, C.; Welsher, K. Real-time 3D single particle tracking: towards active feedback single molecule spectroscopy in live cells. *Molecules* **2019**, *24* (15), 2826.
(14) Hou, S.; Exell, J.; Welsher, K. Real-time 3D single molecule tracking. *Nature Communications* **2020**, *11* (1), 3607. DOI: 10.1038/s41467-020-17444-6.
(15) Johnson, C.; Exell, J.; Lin, Y.; Aguilar, J.; Welsher, K. D. Capturing the start point of the virus–cell interaction with high-speed 3D single-virus tracking. *Nature Methods* **2022**, *19* (12), 1642-1652. DOI: 10.1038/s41592-022-01672-3.
(16) Tan, X.; Welsher, K. Particle-by-Particle In Situ Characterization of the Protein Corona via Real-Time 3D Single-Particle-Tracking Spectroscopy. *Angewandte Chemie International Edition* **2021**, *60* (41), 22359-22367.
(17) Yu, D.; Garcia, A.; Blum, S. A.; Welsher, K. D. Growth Kinetics of Single Polymer Particles in Solution via Active-Feedback 3D Tracking. *Journal of the American Chemical Society* **2022**, *144* (32), 14698-14705. DOI: 10.1021/jacs.2c04990.
(18) Kim, J.; Jozic, A.; Lin, Y.; Eygeris, Y.; Bloom, E.; Tan, X.; Acosta, C.; MacDonald, K. D.; Welsher, K. D.; Sahay, G. Engineering Lipid Nanoparticles for Enhanced Intracellular Delivery of mRNA through Inhalation. *ACS Nano* **2022**, *16* (9), 14792-14806. DOI: 10.1021/acsnano.2c05647.
(19) Wang, Q.; Moerner, W. Optimal strategy for trapping single fluorescent molecules in solution using the ABEL trap. *Applied Physics B* **2010**, *99*, 23-30.
(20) Agnihotri, S. M.; Ohshima, H.; Terada, H.; Tomoda, K.; Makino, K. Electrophoretic Mobility of Colloidal Gold Particles in Electrolyte Solutions. *Langmuir* **2009**, *25* (8), 4804-4807. DOI: 10.1021/la803671t.
(21) Makino, K.; Ohshima, H. Electrophoretic Mobility of a Colloidal Particle with Constant Surface Charge Density. *Langmuir* **2010**, *26* (23), 18016-18019. DOI: 10.1021/la1035745.
(22) Kesler, V.; Murmann, B.; Soh, H. T. Going beyond the Debye Length: Overcoming Charge Screening Limitations in Next-Generation Bioelectronic Sensors. *ACS Nano* **2020**, *14* (12), 16194-16201. DOI: 10.1021/acsnano.0c08622.
(23) Bockenhauer, S. D.; Duncan, T. M.; Moerner, W.; Börsch, M. The regulatory switch of F1-ATPase studied by single-molecule FRET in the ABEL Trap. In *Single Molecule Spectroscopy and Superresolution Imaging VII*, 2014; SPIE: Vol. 8950, pp 65-78.
(24) Dienerowitz, M.; Howard, J. A.; Quinn, S. D.; Dienerowitz, F.; Leake, M. C. Single-molecule FRET dynamics of molecular motors in an ABEL trap. *Methods* **2021**, *193*, 96-106.

(25) Fields, A. P.; Cohen, A. E. Anti-Brownian traps for studies on single molecules. *Methods in enzymology* **2010**, *475*, 149-174.
(26) Tan, X.; Hou, S.; Niver, A.; Zhang, C.; Johnson, A.; Welsher, K. D. Active-feedback 3D single-molecule tracking using a fast-responding galvo scanning mirror. *The Journal of Physical Chemistry A* **2023**, *127* (30), 6320-6328.
(27) Gessner, A.; Lieske, A.; Paulke, B. R.; Müller, R. H. Influence of surface charge density on protein adsorption on polymeric nanoparticles: analysis by two-dimensional electrophoresis. *European Journal of Pharmaceutics and Biopharmaceutics* **2002**, *54* (2), 165-170. DOI: https://doi.org/10.1016/S0939-6411(02)00081-4.
(28) Gessner, A.; Lieske, A.; Paulke, B.-R.; Müller, R. H. Functional groups on polystyrene model nanoparticles: Influence on protein adsorption. *Journal of Biomedical Materials Research Part A* **2003**, *65A* (3), 319-326. DOI: https://doi.org/10.1002/jbm.a.10371.
(29) Wang, H.-X.; Zuo, Z.-Q.; Du, J.-Z.; Wang, Y.-C.; Sun, R.; Cao, Z.-T.; Ye, X.-D.; Wang, J.-L.; Leong, K. W.; Wang, J. Surface charge critically affects tumor penetration and therapeutic efficacy of cancer nanomedicines. *Nano Today* **2016**, *11* (2), 133-144. DOI: https://doi.org/10.1016/j.nantod.2016.04.008.